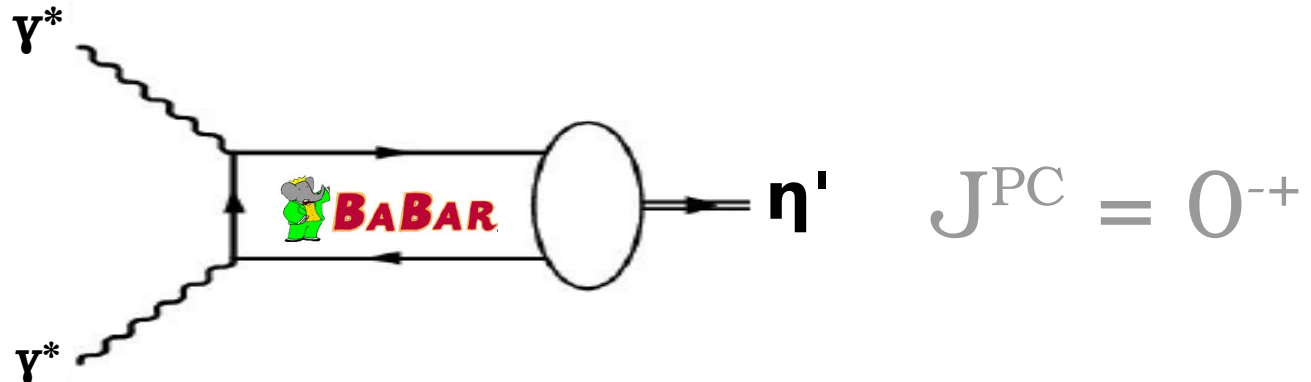


# Pseudoscalar mesons transition form factors (TFF)

## New study of $e^+e^- \rightarrow e^+e^-\eta'$ in the double-tag mode at BABAR

(based on arXiv:1808.08038)

Evgeny Kozyrev, Vladimir Druzhinin



September 28, 2018

# Outline

- Introduction
  - The definition of transition form factor (TFF)*
  - Theoretical aspects*
  - Existing experimental data*
- Measurement of the TFF of  $\eta'$  meson with BaBar detector
- Comparison with theoretical predictions
- Summary
- Prospects for such investigations with VEPP-2000 and c/tau

**M. Poppe, Int. J. Mod. Phys. A 1, 545 (1986):**

At present, a major interest of  $\gamma\gamma$  physics concerns the answer to the question “do the photons resolve the hadron’s structure or not?” In other words: is particle production in  $\gamma\gamma$  interactions primarily the production of quark pairs or is the VDM interpretation correct that the photons turn into vector mesons before they interact? In the latter case, two-photon physics would be just a continuation of fixed target hadron scattering experiments, and we would not expect great news to appear.

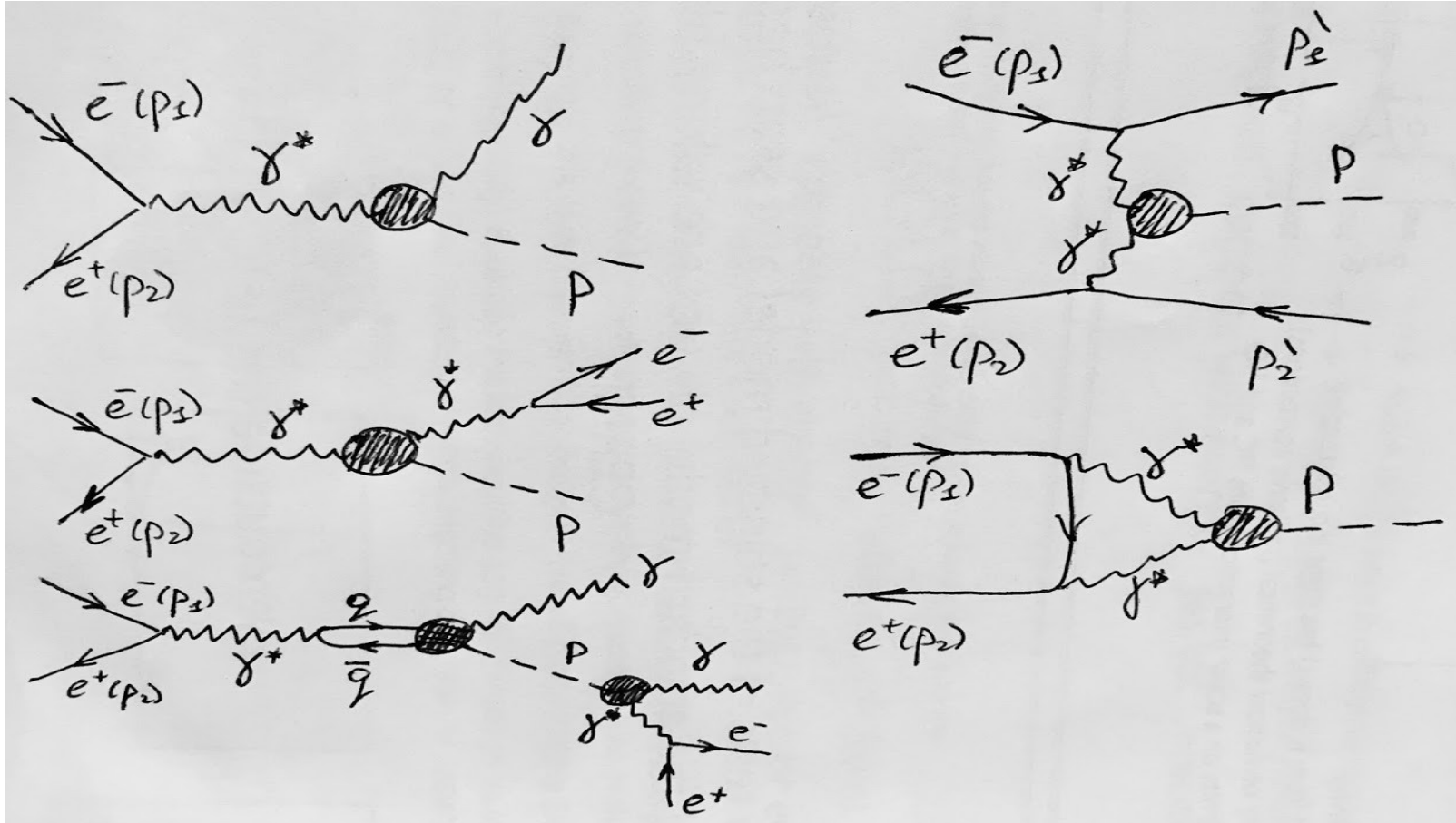
**A.V. Radyushkin, R. Ruskov, Nuclear Physics B 481 (1996) 625-680:**

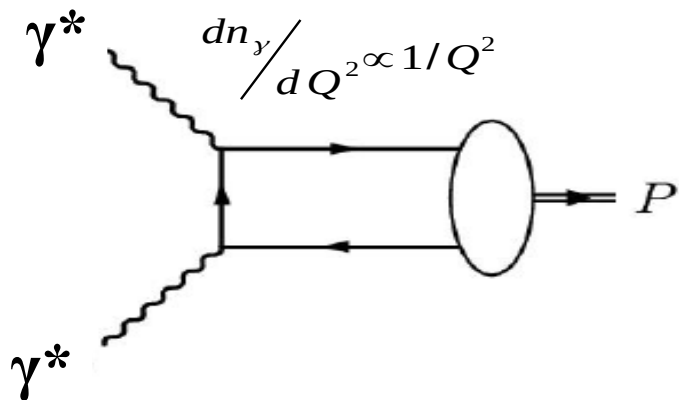
$$F_{\gamma^*\gamma^*\pi^0}^{LO}(q^2, Q^2) = \frac{4\pi}{3} \int_0^1 \frac{\varphi_\pi(x)}{xQ^2 + \bar{x}q^2} dx,$$

	VMD	pQCD
$Q_1^2 \approx 0, Q_2^2 \rightarrow \infty$	$1/Q^2$	$1/Q^2$
$Q_1^2, Q_2^2 \rightarrow \infty$	$1/Q^4$	$1/Q^2$

where  $\varphi_\pi(x)$  is the pion distribution amplitude and  $x, \bar{x} \equiv 1 - x$  are the fractions of the pion light-cone momentum carried by the quarks. In the region where both photon virtualities are large:  $q^2 \sim Q^2 \gtrsim 1 \text{ GeV}^2$ , the pQCD predicts the overall  $1/Q^2$  fall-off of the form factor, which differs from the naive vector meson dominance expectation  $F_{\gamma^*\gamma^*\pi^0}(q^2, Q^2) \sim 1/q^2 Q^2 \sim 1/Q^4$ . Thus, establishing the  $1/Q^2$  power law in this region is a crucial test of pQCD for this process. The study of  $F_{\gamma^*\gamma^*\pi^0}(q^2, Q^2)$  over a wide range of the ratio  $q^2/Q^2$  of two large photon virtualities can then provide non-trivial information about the shape of  $\varphi_\pi(x)$ .

# Examples of experimental setups for the measurement of TFF





$\mathbf{P}$  — pseudoscalar meson

$e_{1,2}$  — photon polarization

$q_{1,2}$  — 4-momentum of photon

$$-Q^2 = q^2$$

### The amplitude of the $\gamma^*\gamma^* \rightarrow \mathbf{P}$ transition:

$$A = e^2 \varepsilon_{\mu\nu\alpha\beta} e_1^\mu e_2^\nu q_1^\alpha q_2^\beta F(q_1^2, q_2^2),$$

- There are a lot of experimental study of pseudoscalar meson production via the fusion of real (**on-shell**) and virtual (**off-shell**) photons

$$\gamma^*\gamma \rightarrow \mathbf{P}: \pi^0, \eta, \eta', \eta_c$$

- There are **no** measurements of the double **off-shell** transitions

$$\gamma^*\gamma^* \rightarrow \mathbf{P}$$

- $\eta'$  decay to real photons:

$$\Gamma_{\eta' \rightarrow 2\gamma} = \frac{\pi\alpha^2 m_{\eta'}^3}{4} |F(0, 0)|^2 = 4.30 \pm 0.16 \text{ keV}$$



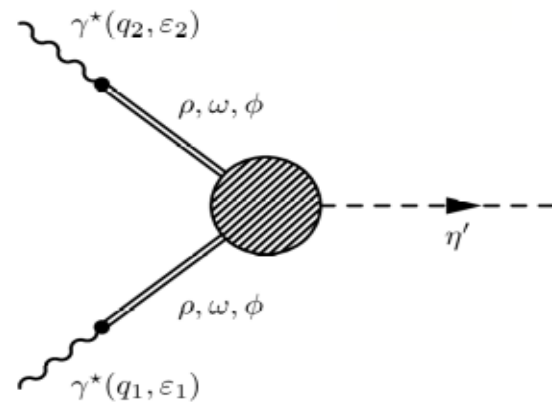
$$F(0, 0) = 0.342 \pm 0.006 \text{ GeV}^{-1}.$$

- The vector meson dominance model is commonly used to describe TFF at low  $Q^2$ :

$$F(Q^2) = \frac{\sum_V \frac{f_{PV\gamma}}{f_V} \cdot \frac{m_V^2}{m_V^2 - q^2 - iW_V m_V} \cdot F(0)}{\sum_V \frac{f_{PV\gamma}}{f_V}}$$

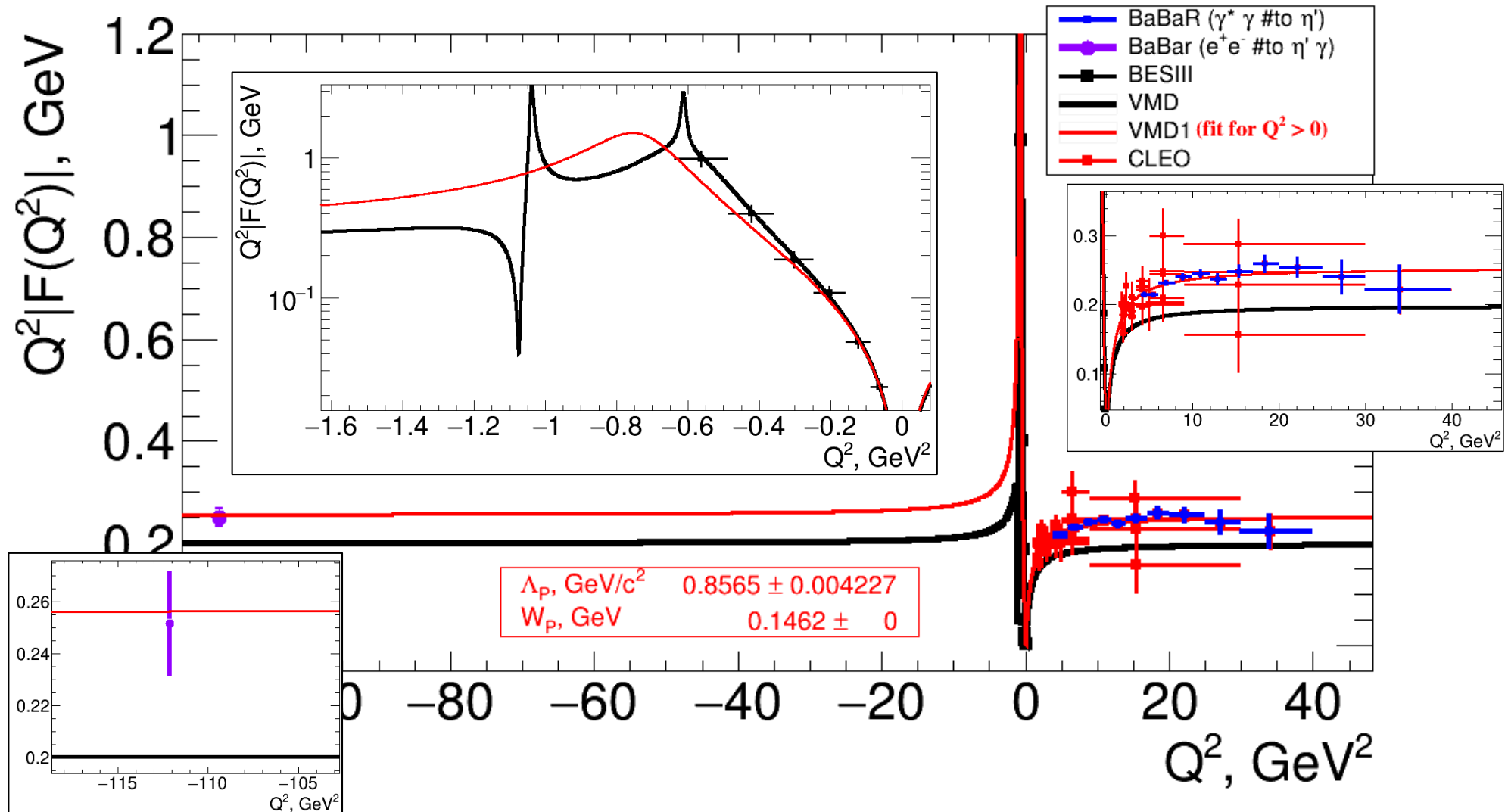


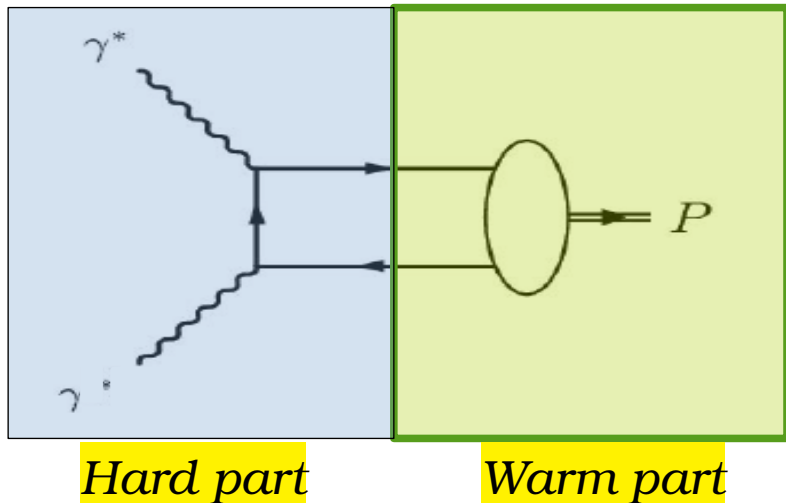
PDG
$W(\eta' \rightarrow \rho\gamma)$
$W(\eta' \rightarrow \omega\gamma)$
$W(\phi \rightarrow \eta'\gamma)$
$W(\phi \rightarrow ee)$
$W(\rho \rightarrow ee)$
$W(\omega \rightarrow ee)$



$$B(\phi \rightarrow \eta'\gamma) = (11, 4_{-4,4}^{+5,4} \pm 2, 0) \cdot 10^{-5}.$$

- In double off-shell case at  $Q^2 > W_V m_V$ :  $F_{\eta'}(Q_1^2, Q_2^2) = \frac{F_{\eta'}(0, 0)}{(1 + Q_1^2/\Lambda_P^2)(1 + Q_2^2/\Lambda_P^2)}$   
 where  $\Lambda_P$  — effective pole mass parameter





$$F(\mathcal{Q}_1^2, \mathcal{Q}_2^2) = \int \mathbf{T}(\mathbf{x}, \mathcal{Q}_1^2, \mathcal{Q}_2^2) \boldsymbol{\varphi}(\mathbf{x}, \mathcal{Q}_1^2, \mathcal{Q}_2^2) d\mathbf{x}$$

$x$  - is the fraction of the meson momentum carried by one of the quarks

$\mathbf{T}(\mathbf{x}, \mathcal{Q}_1^2, \mathcal{Q}_2^2)$  - hard scattering amplitude for  $\gamma^* \gamma^* \rightarrow q\bar{q}$  transition which is calculable in pQCD

$\boldsymbol{\varphi}(\mathbf{x}, \mathcal{Q}_1^2, \mathcal{Q}_2^2)$  - nonperturbative meson distribution amplitude (DA) describing transition  $P \rightarrow q\bar{q}$

$$T_H(x, Q_1^2, Q_2^2) = \frac{1}{2} \cdot \frac{1}{xQ_1^2 + (1-x)Q_2^2} \cdot \left( 1 + C_F \frac{\alpha_S(Q^2)}{2\pi} \cdot t(x, Q_1^2, Q_2^2) \right) + (x \rightarrow 1-x) + O(\alpha_s^2) + O(\Lambda_{QCD}^4/Q^4)$$

**NLO correction** [E. Braaten, Phys. Rev. D **28**, 3 (1983)]

- The shape ( $x$  dependence) of meson DA  $\boldsymbol{\varphi}(\mathbf{x}, \mathcal{Q}_1^2, \mathcal{Q}_2^2)$  is unknown, but its evolution with  $\mu^2 = \mathcal{Q}_1^2 + \mathcal{Q}_2^2$  is predicted by pQCD:

At the limit  $\mu \rightarrow \infty$

$$\mu^2 \frac{d}{d\mu^2} \phi(x, \mu) = \frac{\alpha_s(\mu)}{2\pi} \int_0^1 dy V(x, y) \phi(y, \mu)$$

$$\phi_P(x, \mu) = A_P 6x(1-x) (1 + O(\Lambda_{QCD}^2/\mu^2))$$

[S. J. Brodsky and G. P. Lepage, Phys. Rev. D **24**, 7 (1981)]

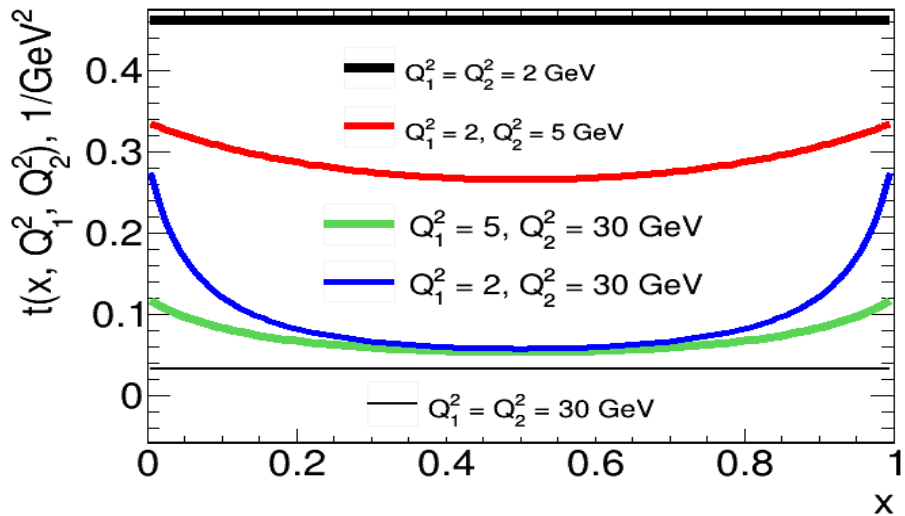


$$F_{\eta'}(Q_1^2, Q_2^2) = \left( \frac{5\sqrt{2}}{9} f_n \sin \phi + \frac{2}{9} f_s \cos \phi \right) \int_0^1 dx \frac{1}{2} \frac{6x(1-x)}{xQ_1^2 + (1-x)Q_2^2} \left( 1 + C_F \frac{\alpha_s(\mu^2)}{2\pi} \cdot t(x, Q_1^2, Q_2^2) \right) + (x \rightarrow 1-x),$$

NLO

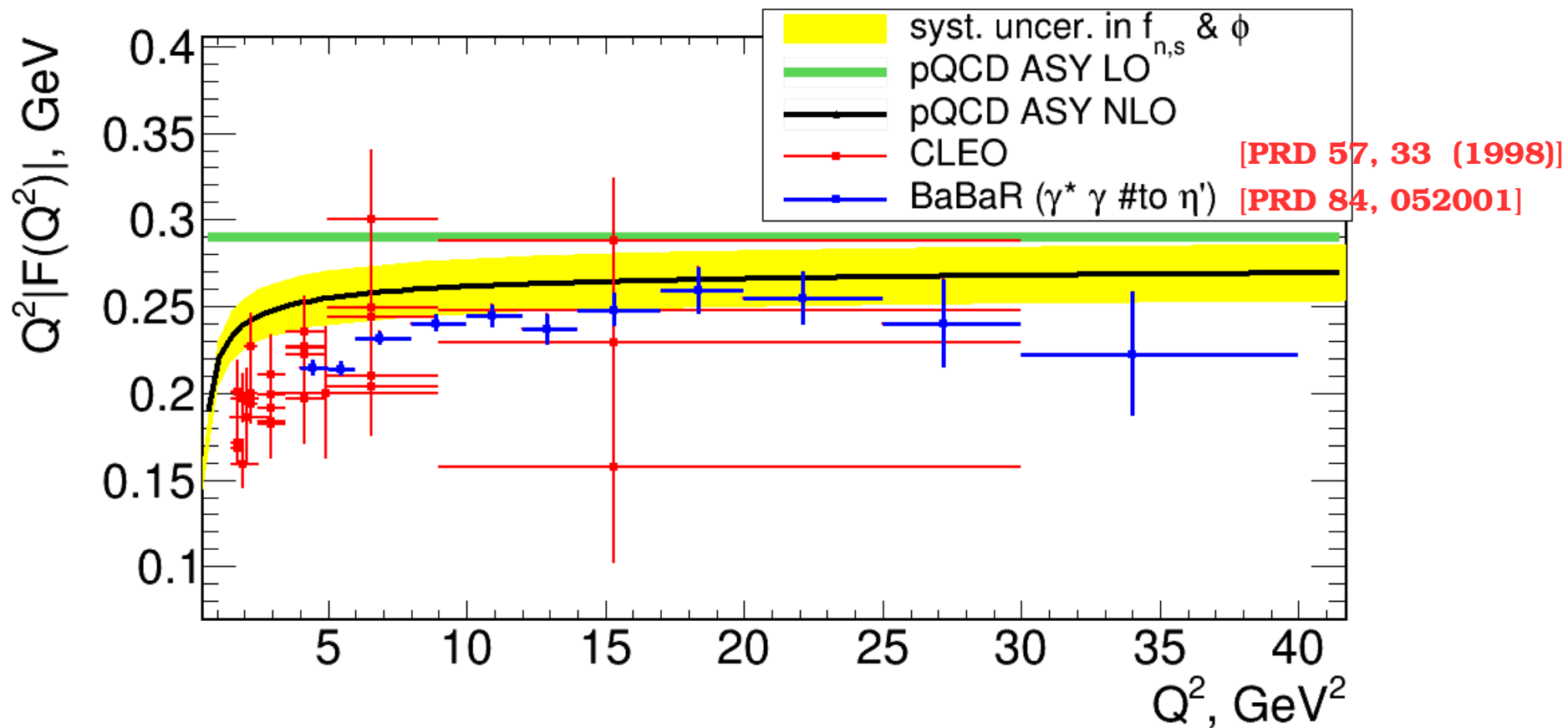
Master formula

The meson DA



- The double-virtual TFF is **less sensitive to NLO** than the single off-shell TFF.

- The form  $1/[xQ_1^2 + (1-x)Q_2^2]$  is not divergent, so double off-shell transition FF is **less sensitive to a shape of the meson DA** in comparison to the single off-shell FF.



*The  $\gamma^*\gamma \rightarrow \eta$  Transition Form Factor*

**Pseudoscalar pole contribution to the hadronic light-by-light piece of  $a_\mu$**

**Adolfo Guevara, Pablo Roig, JJ Sanz Cillero. Sep 17, 2018. 7 pp.**

**Conference: C18-06-25.2**

**e-Print: [arXiv:1809.06175](https://arxiv.org/abs/1809.06175)**

is the largest one. A way to reduce such uncertainty could be by taking into account data from doubly off-shell TFF such as that given by BaBar for the  $\eta'$ -TFF [35]. Considering all possible contributions to the error we get

$$a_\mu^{P,HLbL} = (8.47 \pm 0.16_{\text{sta}} \pm 0.09_{1/N_C} \pm 0.5_{\text{asym}}) \cdot 10^{-10}, \quad (14)$$

where the first error (sta) comes from the fit of the TFF, the second from possible  $1/N_C$  corrections and the last from the wrong asymptotic behavior estimated through the effects of heavier resonances in the TFF.

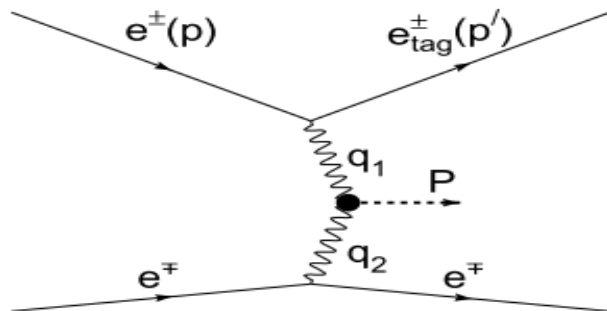
The analysis is based on the previous BaBar study [1].

### Previous

$$\gamma\gamma^* \rightarrow \eta'$$

Single tagged

~ 5000 signal events

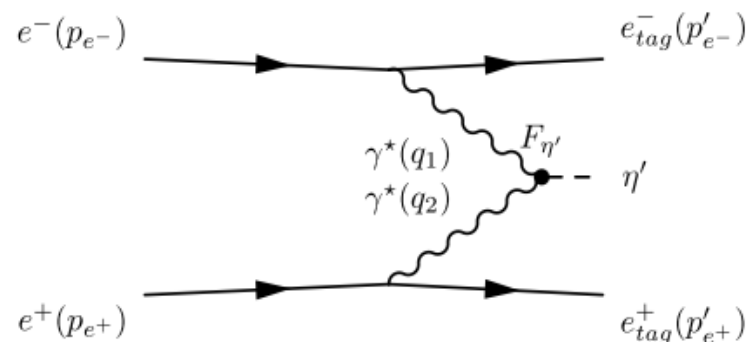


### New

$$\gamma^*\gamma^* \rightarrow \eta'$$

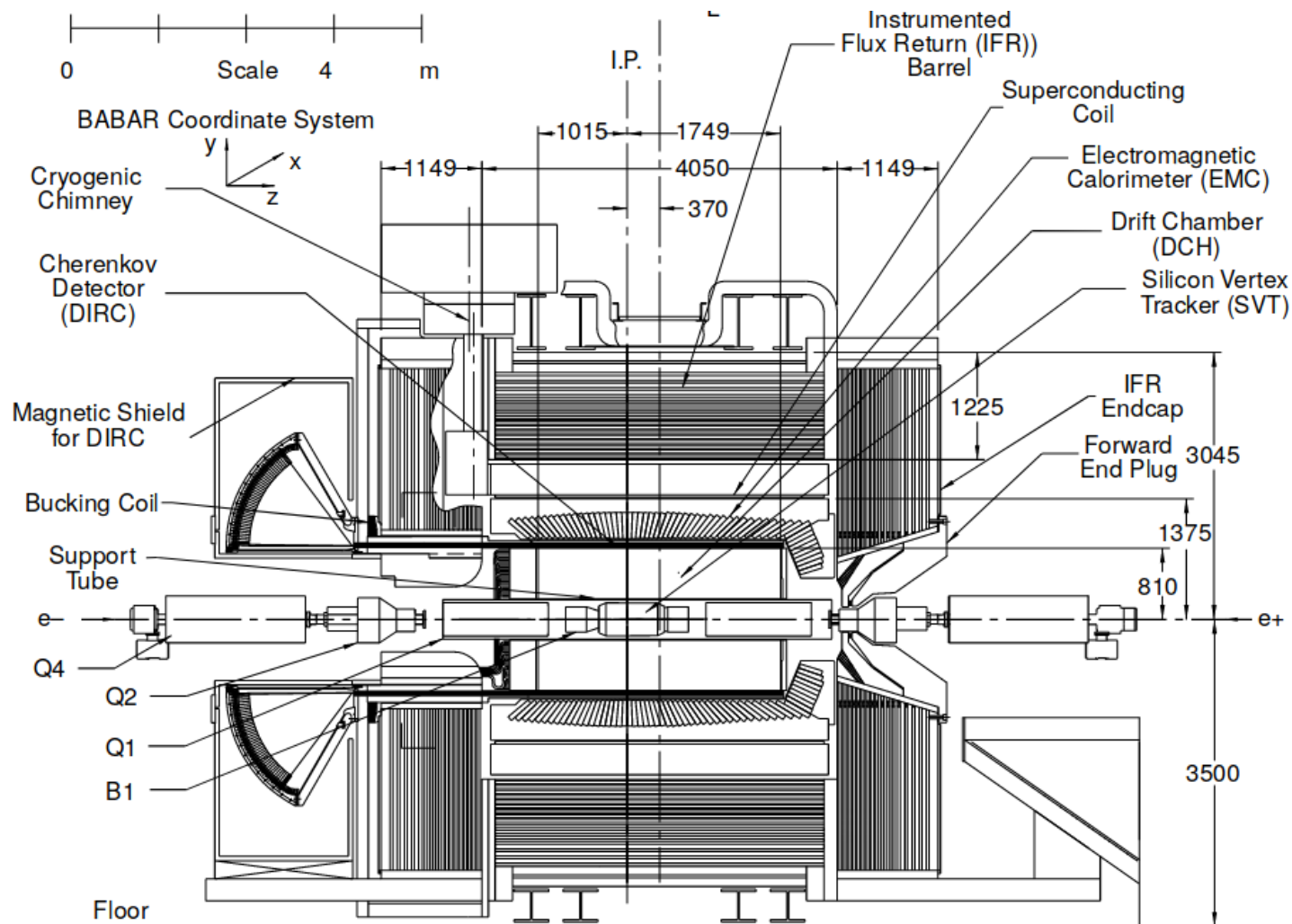
Double tagged

$46^{+8}_{-7}$  signal events

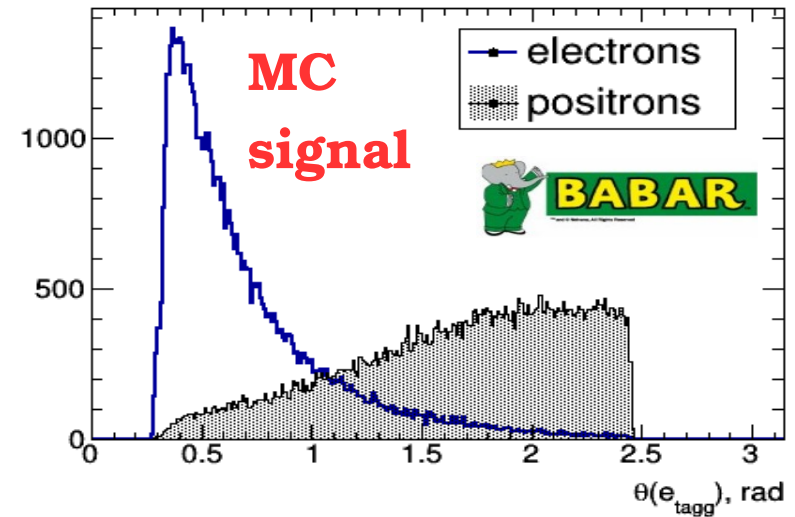
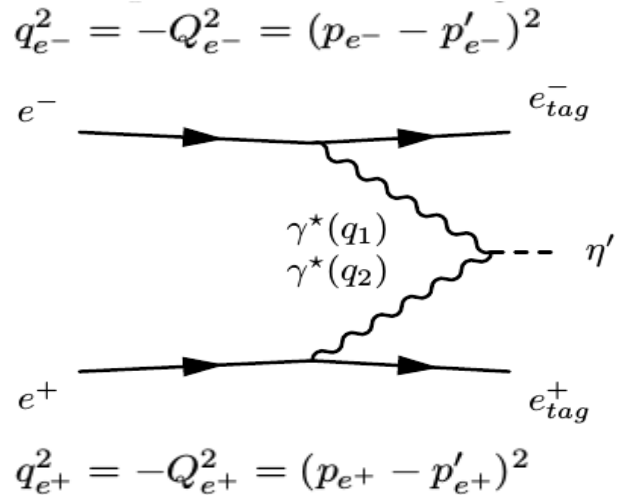


- A large number of systematic uncertainties were studied in our previous work where the number of signal events was significantly larger.

[1] [PRD 84, 052001]: P. del Amo Sanchez *et al.* (BaBar collaboration), *Phys. Rev. D* 84, 052001 (2011) — (126 citations).



# Technique



*Polar angle distribution for tagged electrons  
(positrons)*

- The decay chain  $\eta' \rightarrow \pi^+ \pi^- \eta \rightarrow \pi^+ \pi^- 2\gamma$  is used
- A total integrated luminosity  $L = 469 \text{ fb}^{-1}$
- GGResRc event generator is used [[arXiv:1010.5969](https://arxiv.org/abs/1010.5969)]. Initial and final state radiative corrections as well as vacuum polarization effects are included. The form factor is fixed to the constant value  $F(0,0)$ .

**The strategy:**  $dN/dQ^2 \longrightarrow d\sigma/dQ^2 \longrightarrow |F(Q^2)|$

We require the presense

- at least **two tracks** from *GoodTrackLoose* list passed *LooseElectronMicroSecection*

- at least **two tracks** from *GoodTrackLoose* list passed *TightKMPionMicroSelection*

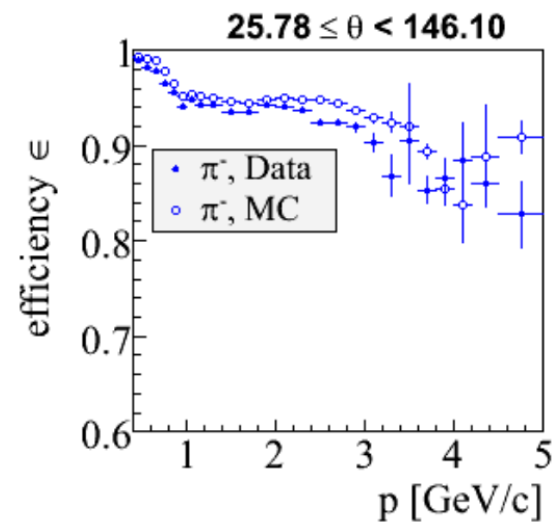
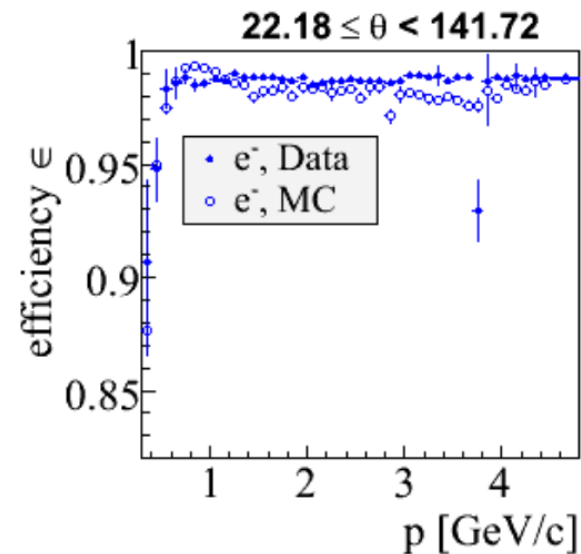
- at least **two photons** from *GoodPhotonLoose* list

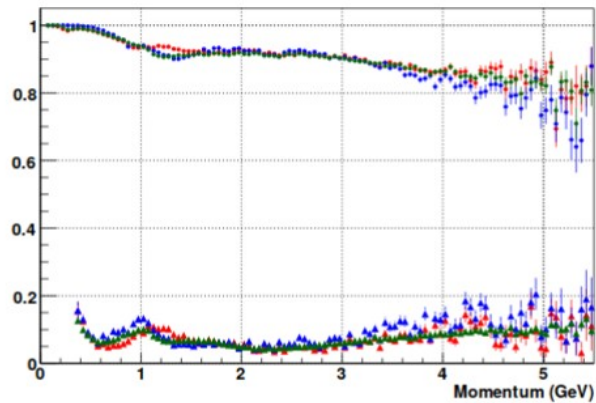
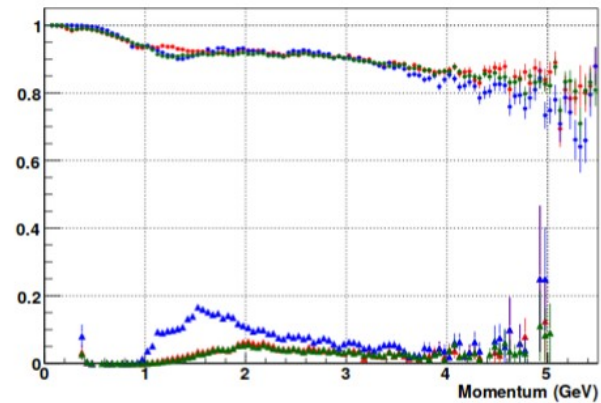
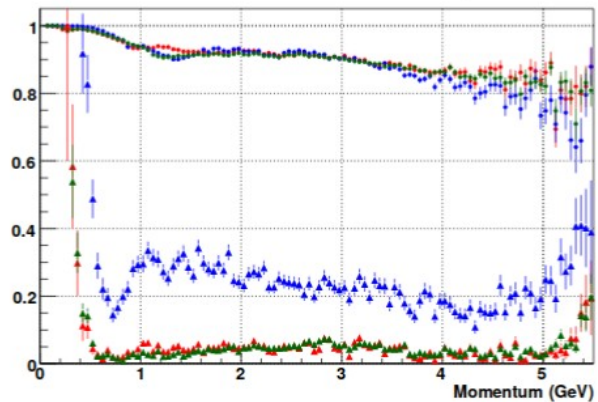
$$-\varepsilon_{\gamma} > 30 \text{ MeV}$$

$$-0.45 < m_{\gamma\gamma} < 0.65 \text{ GeV}/c^2$$

- The photon candidates are fitted with a  $\eta$  mass constraint.

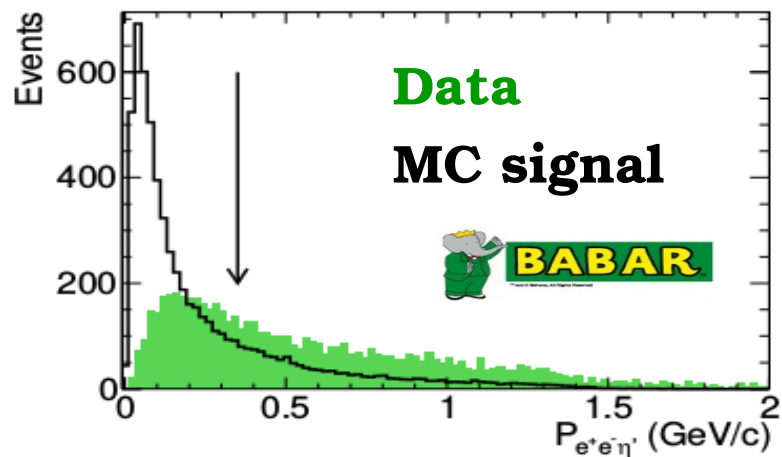
- The  $\eta$  candidate and a pair of oppositely-charged pion candidates are fitted with a  $\eta'$  mass constraint.



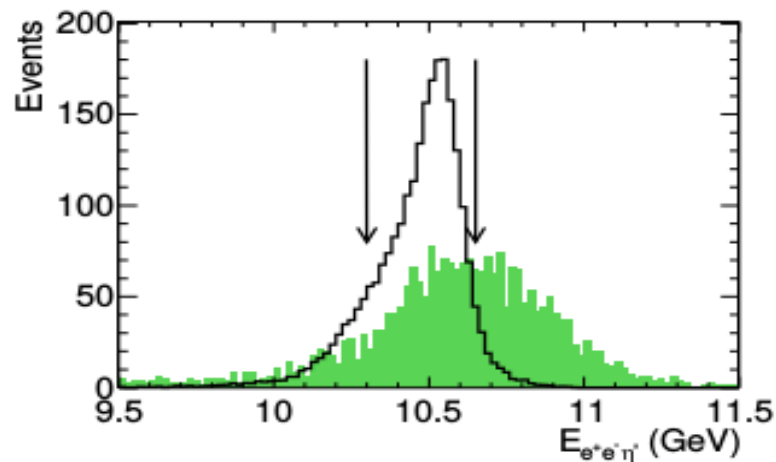
Pions misidentification with *TightKMPionMicroSelection*:pipi- $\pi$ Tight misid\* 1.0 KMTight-Red, LHTight-Blue, oldKMTight-Green(a)  $K$  as  $\pi$  mis-id\*1pipi- $p$ Tight misid\* 1.0 KMTight-Red, LHTight-Blue, oldKMTight-Green(b)  $p$  as  $\pi$  mis-id\*1pipi- $\pi$ Tight misid\* 5.0 KMTight-Red, LHTight-Blue, oldKMTight-Green



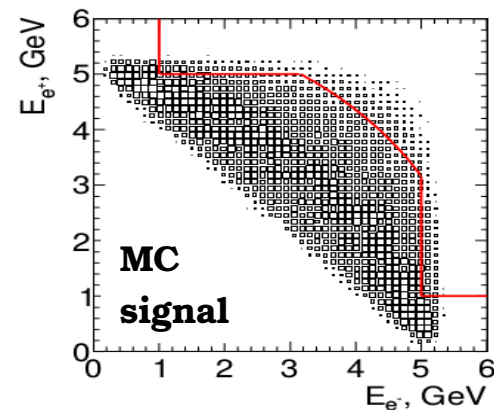
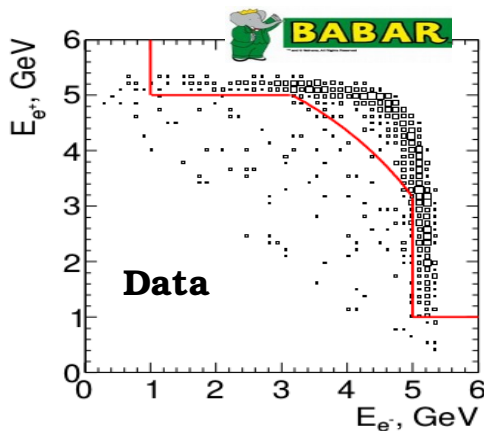
- $P_{\text{c.m.}}(e^+e^-\pi^+\pi^-\eta) < 0.35 \text{ GeV}/c$ .



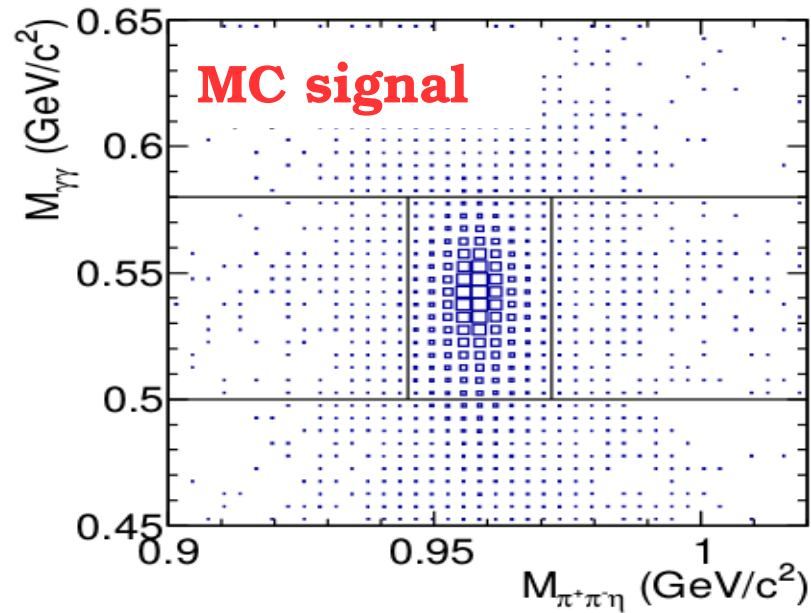
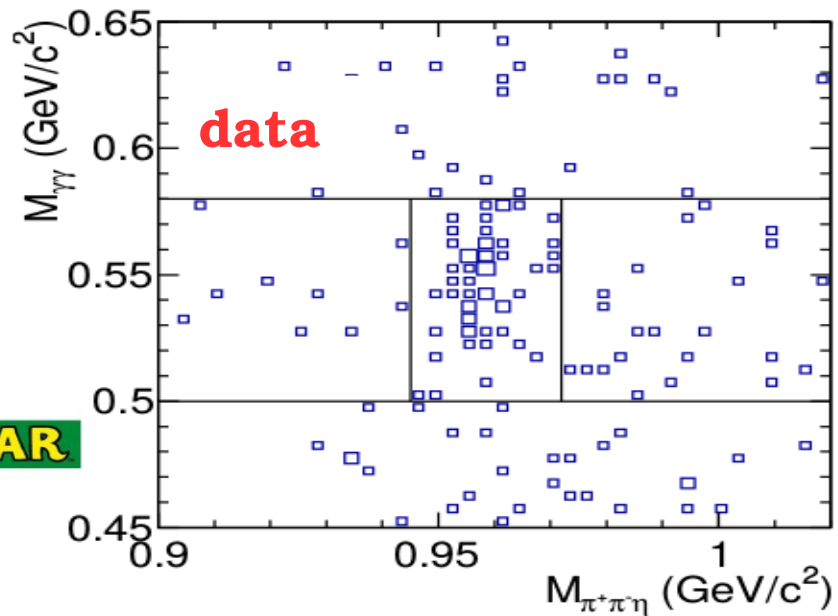
- $10.3 < E_{\text{c.m.}}(e^+e^-\pi^+\pi^-\eta) < 10.7 \text{ GeV}$



- Events that lie above and on the right of the lines (mostly, Bhabha scattering) are rejected.



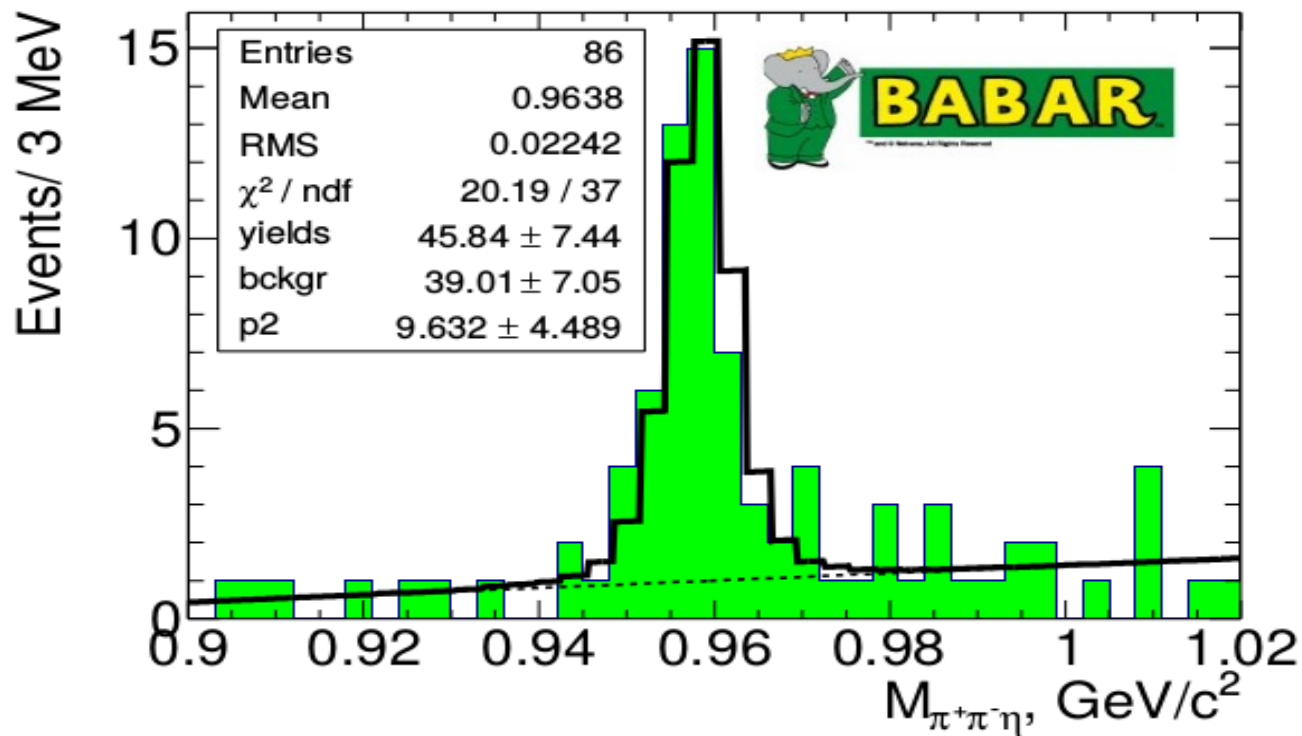
*The positron c.m. energy vs the electron c.m. energy*



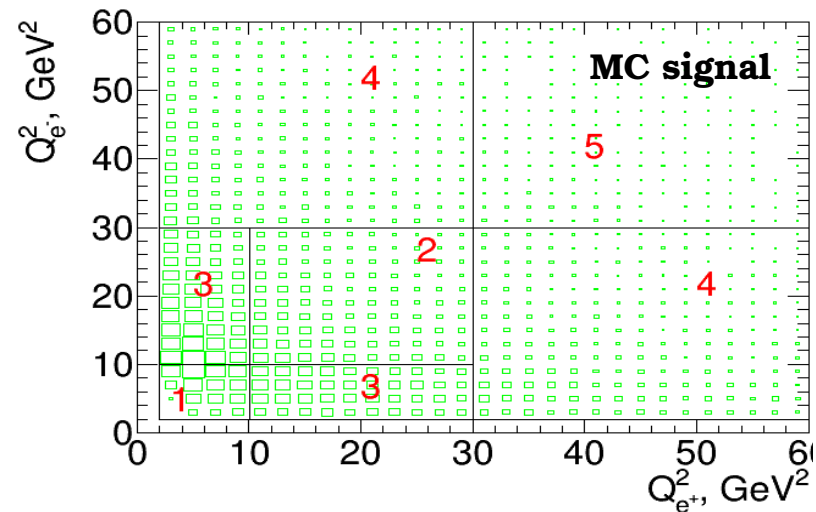
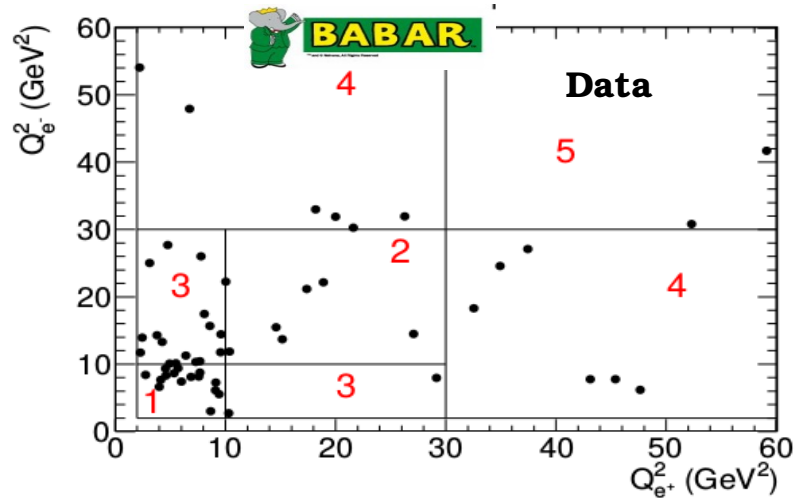
$m_{\gamma\gamma}$  vs.  $m_{\pi^+\pi^-\eta}$

- We require  $0.50 < m_{\gamma\gamma} < 0.58$  GeV/c<sup>2</sup>





The  $\pi^+\pi^-\eta$  mass spectra for data events. The open histogram is the fit result. The dashed line represents fitted background.



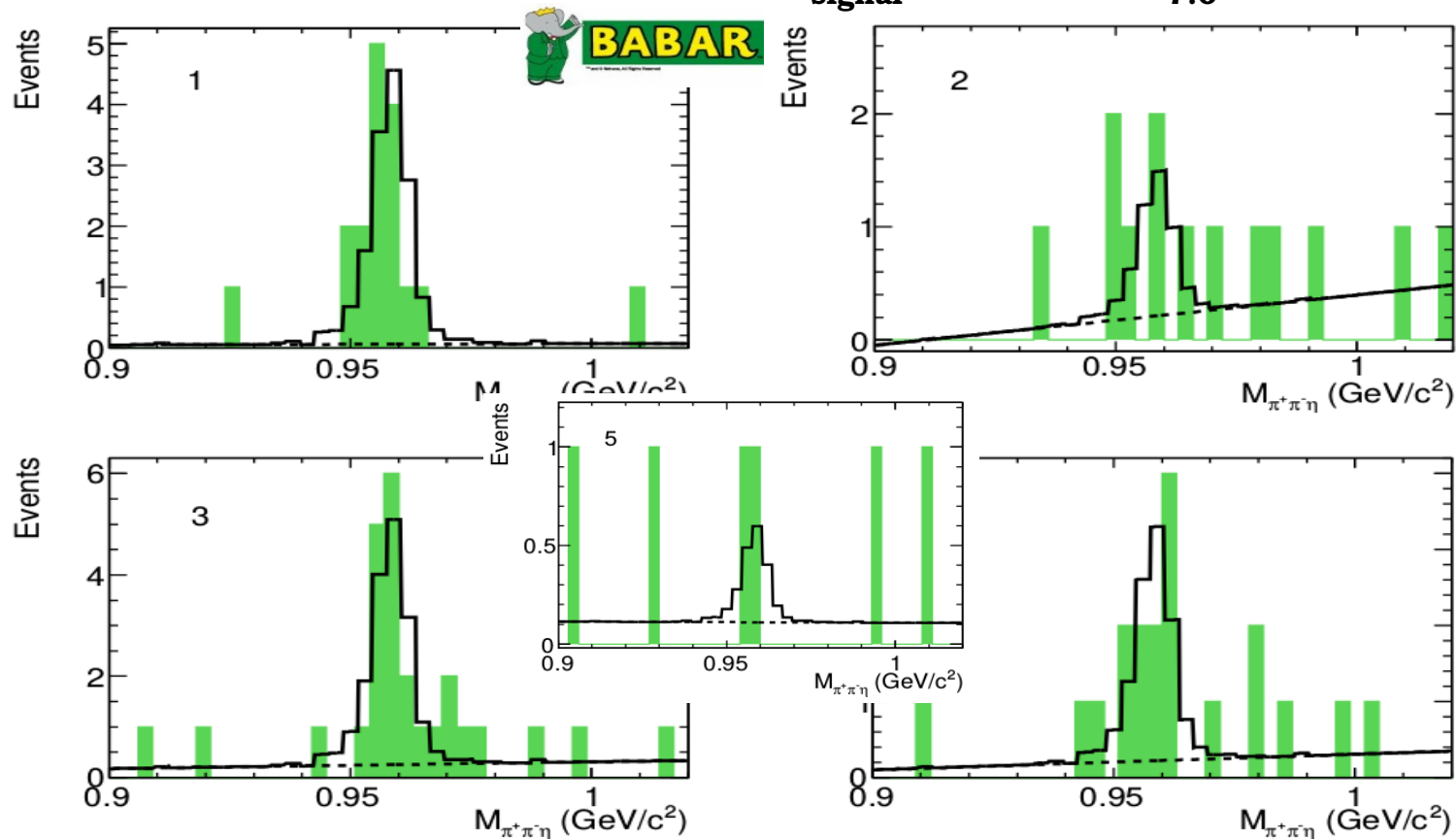
The  $Q_{e-}^2$  vs.  $Q_{e+}^2$  for events with  $0.945 < m_{2\pi\eta} < 0.972$  GeV/c<sup>2</sup>

- New definition:  $Q_1^2 = \max(Q_{e+}^2, Q_{e-}^2)$ ,  $Q_2^2 = \min(Q_{e+}^2, Q_{e-}^2)$

- The average momentum transfers for each region are calculated using the data spectrum **normalized to the detection efficiency**:

$$\overline{Q_{1,2}^2} = \frac{\sum_i Q_{1,2}^2(i) / \epsilon(Q_1^2, Q_2^2)}{\sum_i 1 / \epsilon(Q_1^2, Q_2^2)}$$

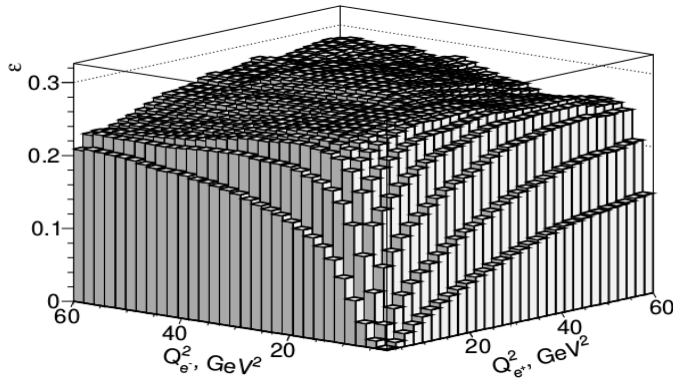
- The total number of signal events  $N_{\text{signal}}^{\text{fit}} = 46.2^{+8.3}_{-7.0}$



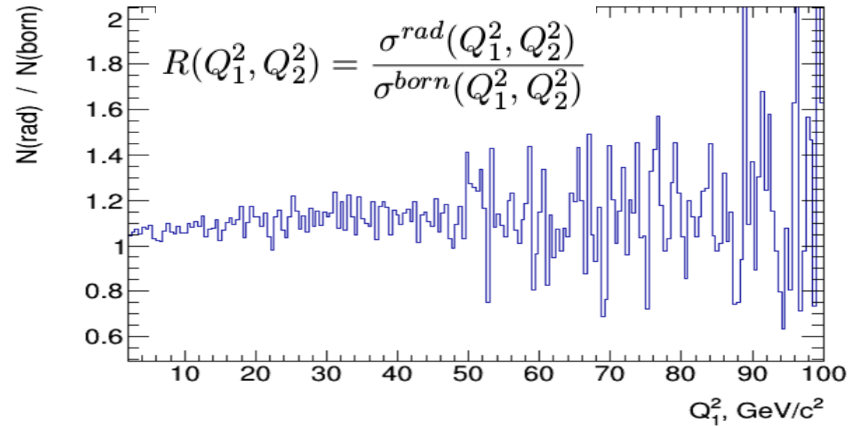
*The  $\pi^+\pi^-\eta$  mass spectra for data events for the five  $Q^2$  ranges. The open histograms are the fit results. The dashed lines represent background.*

- The detector acceptance limits the  $e^-e^+$  detection efficiency at small  $Q^2$ . The minimum  $Q^2$  equals to  $2 \text{ GeV}^2$ .

$$\epsilon_{true} = \frac{\int \epsilon(Q_1^2, Q_2^2) F_{\eta'}^2(Q_1^2, Q_2^2) dQ_1^2 dQ_2^2}{\int F_{\eta'}^2(Q_1^2, Q_2^2) dQ_1^2 dQ_2^2} \quad (\mathbf{F}_{\eta'} \text{ from master formula at slide \#7})$$



The dependence of detection efficiency on momentum transfers.



The ratio of generated spectra with rad. photons vs. without photons

- R leads to the decrease of the detection efficiency by  $\sim 10 \%$ .
- The maximum energy of the photon emitted from the initial state is restricted by the requirement  $E_\gamma < 0.05\sqrt{s}$ , where  $\sqrt{s}$  is the  $e^+e^-$  center-of-mass (c.m.) energy.

- The differential cross section for  $e^+e^- \rightarrow e^+e^-\eta'$  is calculated as

$$\frac{d^2\sigma}{dQ_1^2 dQ_2^2} = \frac{1}{\epsilon_{\text{true}} R L B} \frac{d^2 N}{dQ_1^2 dQ_2^2}$$

$$F^2(\overline{Q_1^2}, \overline{Q_2^2}) = \frac{(d^2\sigma/(dQ_1^2 dQ_2^2))_{\text{data}}}{(d^2\sigma/(dQ_1^2 dQ_2^2))_{\text{MC}}} F_{\eta'}^2(\overline{Q_1^2}, \overline{Q_2^2})$$

- $B = B(\eta' \rightarrow \pi^+\pi^-\eta) \times B(\eta \rightarrow 2\gamma) = (0.3941 \pm 0.0020) \times (0.429 \pm 0.007) = 0.169 \pm 0.003$

- $\sigma_{e^+e^- \rightarrow e^+e^-\eta'} (2 < Q_1^2, Q_2^2 < 60 \text{ GeV}^2) = (11.4^{+2.8}_{-2.4}) \text{ fb}$

$\overline{Q_1^2}, \overline{Q_2^2}, \text{ GeV}^2$	$\epsilon_{\text{true}}$	$R$	$N_{\text{events}}$	$d^2\sigma/(dQ_1^2 dQ_2^2) \times 10^4, \text{ fb/GeV}^4$	$F(\overline{Q_1^2}, \overline{Q_2^2}) \times 10^3, \text{ GeV}^{-1}$
6.48, 6.48	0.019	1.03	$14.7^{+4.3}_{-3.6}$	$1471.8^{+430.1}_{-362.9}$	$14.32^{+1.95}_{-1.89} \pm 0.83 \pm 0.14$
16.85, 16.85	0.282	1.10	$4.1^{+2.7}_{-2.7}$	$4.2^{+2.8}_{-2.8}$	$5.35^{+1.54}_{-1.54} \pm 0.31 \pm 0.42$
14.83, 4.27	0.145	1.07	$15.8^{+4.8}_{-4.0}$	$39.7^{+12.0}_{-10.2}$	$8.24^{+1.16}_{-1.13} \pm 0.48 \pm 0.65$
38.11, 14.95	0.226	1.11	$10.0^{+3.9}_{-3.2}$	$3.0^{+1.2}_{-1.0}$	$6.07^{+1.09}_{-1.07} \pm 0.35 \pm 1.21$
45.63, 45.63	0.293	1.22	$1.6^{+1.8}_{-1.1}$	$0.6^{+0.7}_{-0.6}$	$8.71^{+3.96}_{-8.71} \pm 0.50 \pm 1.04$

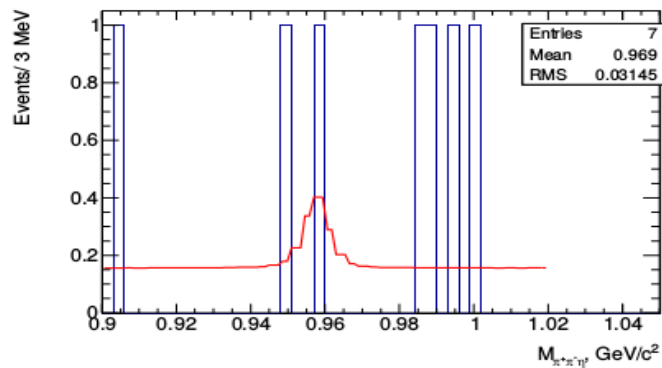
Statistical

Systematic

Model

- The statistical uncertainty is dominant

- $e^+e^- \rightarrow e^+e^-\eta'\pi^0 \rightarrow e^+e^-\pi^+\pi^-\eta\pi^0$  - kinematically closest background for the process under study. Using the simulation of the  $e^+e^- \rightarrow e^+e^-a_0(1450) \rightarrow e^+e^-\eta'\pi^0$  process we estimate the contribution  $N_{\eta'\pi^0} < 0.16$  at 90% C.L.



$$\Rightarrow N_{\eta'\pi^0}^{signal} < 1.45 \text{ at } 90\% \text{ C.L.}$$

The  $\pi^+\pi^-\eta$  invariant mass spectrum

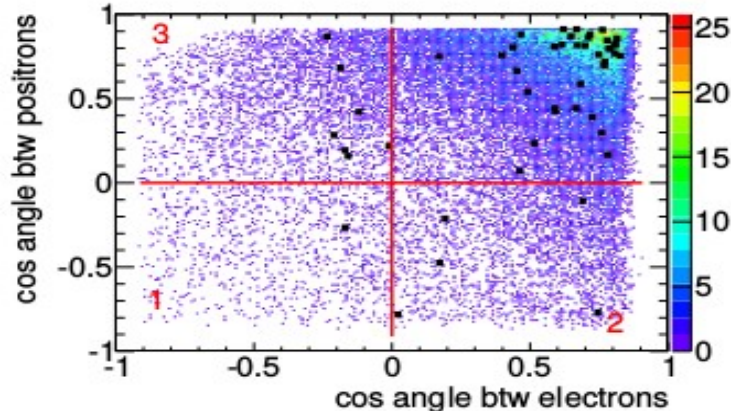
The detection efficiency for  $e^+e^-\eta'\pi^0$  events to pass the selections of  $e^+e^-\eta'$ .

$$N_{bkgr} = \frac{N_{\eta'\pi^0}^{signal} \epsilon_{\eta'\pi^0}^{(2)}}{\epsilon_{\eta'\pi^0}^{(1)}} < 0.16 \text{ at } 90\% \text{ C.L.}$$

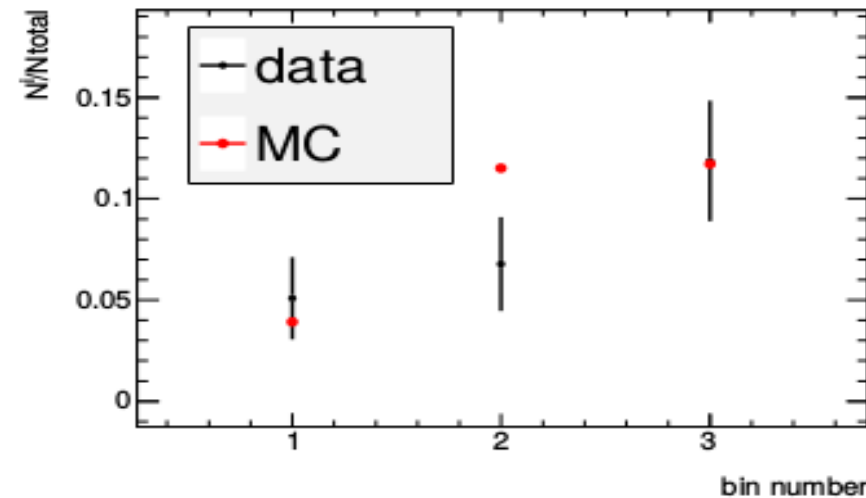
The detection efficiency for  $e^+e^-\eta'\pi^0$  events to pass the selections of  $e^+e^-\eta'\pi^0$ .



- $e^+e^- \rightarrow e^+e^- J/\psi(\phi) \rightarrow e^+e^- \eta' \gamma$  is negligible according to [PRD 84, 052001].
- $e^+e^- \rightarrow \gamma^* \rightarrow X$ :



*The cosine of angle between scattered and initial electron (positron) in c.m.f.*



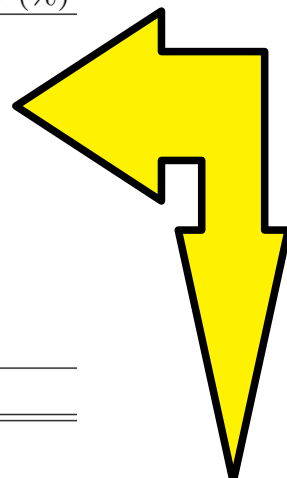
*The fraction of the events in the bins.*

It is reasonable to assume that the  $\cos(\alpha_{e^\pm})$  spectrums must be **symmetric in  $[-1:1]$  region for annihilation processes**, while signal scattered electron (positron) prefers to fly in the about the same direction.

The main source of systematic uncertainty of cross section

Source	Uncertainty (%)
$\pi^\pm$ identification	1.0
$e^\pm$ identification	1.0
Other selection criteria	11
Track reconstruction	0.9
$\eta \rightarrow 2\gamma$ reconstruction	2
Trigger, filters	1.3
Background subtraction	3.7
Radiative correction	1.0
Luminosity	1.0
Total	12%

 from previous BaBar study of  $\gamma^*\gamma \rightarrow \eta'$   
 [PRD 84, 052001]



selection	$N_{signal}/\epsilon_{true}$	deviation from standard criteria
standard selection criteria	$985 \pm 197$	
$P_{e^+e^-\eta'}$ is less than 1 GeV/c instead of 0.35 GeV/c	$1052 \pm 273$	6.8
$10.20 < E_{e^+e^-\eta'} < 10.75$ GeV instead of $10.3 < E_{e^+e^-\eta'} < 10.65$ GeV	$942 \pm 235$	-4.3
without the restrictions on $E_{e^+}$ and $E_{e^-}$	$1061 \pm 280$	7.7
$0.48 < m_{2\gamma} < 0.60$ GeV/c <sup>2</sup> instead of $0.50 < m_{2\gamma} < 0.58$ GeV/c <sup>2</sup>	$958 \pm 181$	-2.7
total		11

- $(d^2\sigma/(dQ_1^2 dQ_2^2))_{MC}$  and  $\epsilon_{true}$  depends on model.

Repeating the calculations with a constant TFF we estimate the model uncertainty.

For the cross section - about 60% due to the strong dependence of  $\epsilon_{true}$  on the input model for TFF at small values of  $Q_1^2$  and  $Q_2^2$ .

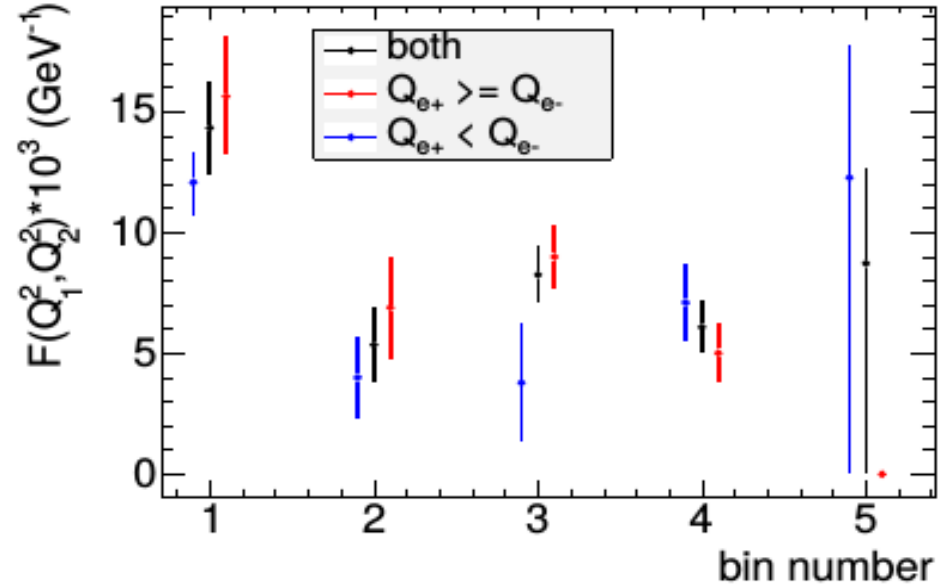
The TFF is much less sensitive to the model.

TABLE V:  $\frac{d^2\sigma}{dQ_1^2 dQ_2^2}$  obtained with different models for TFF

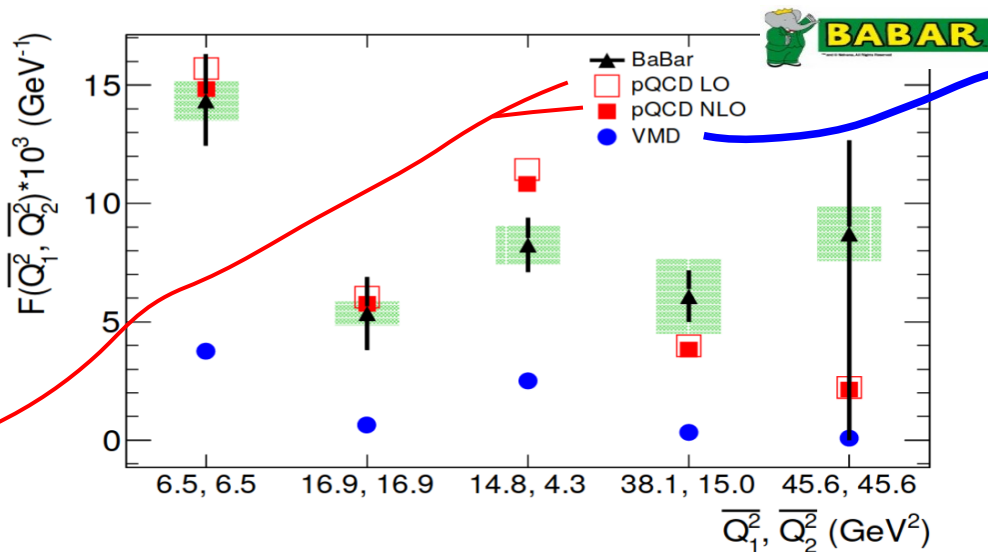
	1	2	3	4	5
QCD	$1471.8^{+430.136}_{-362.91}$	$4.17^{+2.75}_{2.75}$	$39.72^{+11.98}_{-10.18}$	$2.98^{+1.17}_{-0.96}$	$0.62^{+0.69}_{-0.62}$
const	$637.10^{+186.19}_{-157.09}$	$4.15^{+2.74}_{2.74}$	$33.30^{+10.05}_{-8.54}$	$2.76^{+1.08}_{-0.89}$	$0.62^{+0.69}_{-0.62}$
deviation, %	60	0.6	15	7	1.

TABLE VI: TFF obtained with different models for TFF

	1	2	3	4	5
QCD	$14.32^{+1.95}_{-1.89}$	$5.35^{+1.54}_{-1.54}$	$8.24^{+1.16}_{-1.13}$	$6.07^{+1.09}_{-1.07}$	$8.71^{+3.96}_{-8.71}$
const	$14.61^{+1.99}_{-1.92}$	$5.62^{+1.62}_{-1.62}$	$7.24^{+1.02}_{-0.99}$	$7.24^{+1.30}_{-1.28}$	$10.02^{+4.55}_{-10.02}$
deviation %	1	8	8	20	12



The comparison of the measured  $\eta'$  TFF with  $Q_{e^+} < Q_{e^-}$ ,  $Q_{e^+} \geq Q_{e^-}$  and without the restriction.



$$F_{\eta'}(Q_1^2, Q_2^2) = \frac{F_{\eta'}(0, 0)}{(1 + Q_1^2/\Lambda_P^2)(1 + Q_2^2/\Lambda_P^2)}$$

The  $\Lambda_P$  is fixed at 849 MeV/c<sup>2</sup> from the approximation of  $F_{\eta'}(Q^2, 0)$  with one off-shell photon [Phys. Rev. D 85, 057501 (2012)].

The comparison of obtained form-factor with theoretical predictions. Error bars - statistical uncertainties. Shaded rectangles - quadratic sum of the systematic and model uncertainties.

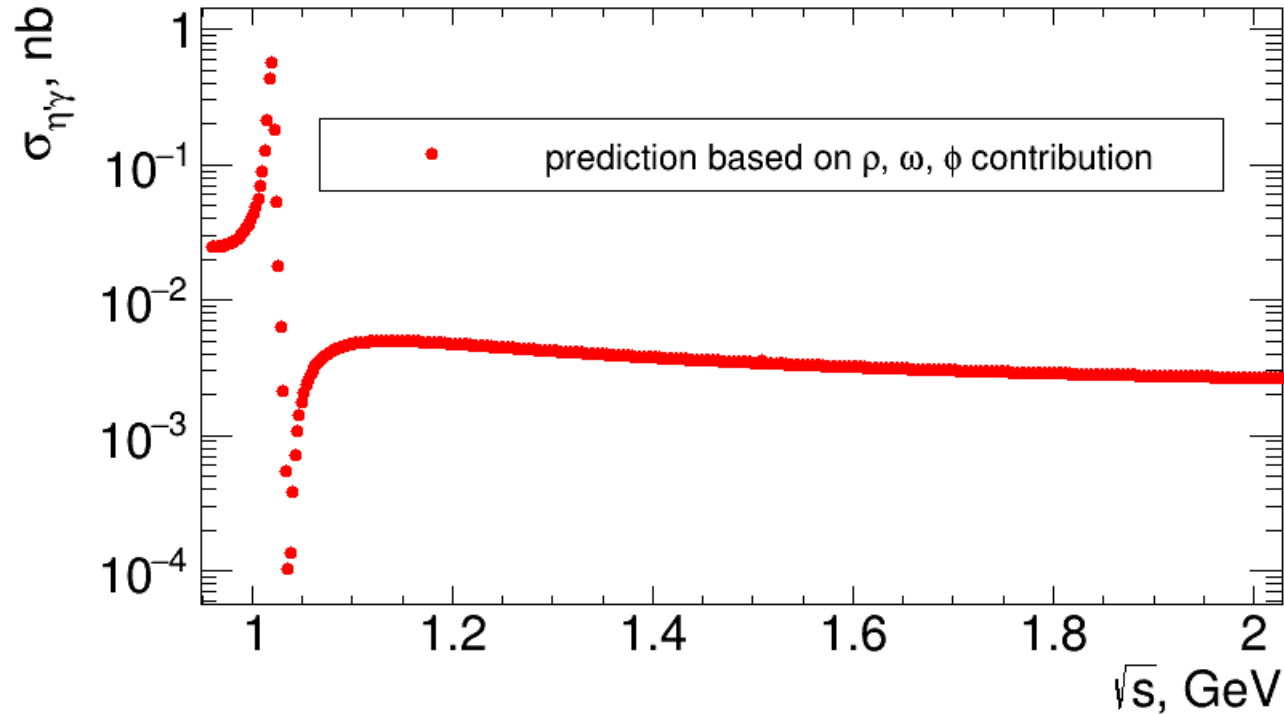
$$F_{\eta'}(Q_1^2, Q_2^2) = \left( \frac{5\sqrt{2}}{9} f_n \sin \phi + \frac{2}{9} f_s \cos \phi \right) \int_0^1 dx \frac{1}{2} \frac{6x(1-x)}{xQ_1^2 + (1-x)Q_2^2} \left( 1 + C_F \frac{\alpha_s(\mu^2)}{2\pi} \cdot t(x, Q_1^2, Q_2^2) \right) + (x \rightarrow 1-x),$$

- pQCD calculation is in good agreement with data ( $\chi^2/\text{n.d.f.} = 6.2/5$ , Prob = 28%)
- VMD model exhibits a clear disagreement with the experiment.



- About 46 events of  $e^+e^- \rightarrow e^+e^-\eta'$  were observed in the double tagged mode for the first time.
- The  $\gamma^*\gamma^* \rightarrow \eta'$  transition form factor  $F(Q^2_1, Q^2_2)$  have been measured for  $Q^2$  range from 2 to 60  $\text{GeV}^2$ .
- The form factor is in reasonable agreement with the pQCD prediction.
- We propose a measurement of this quantity at BELLE II.

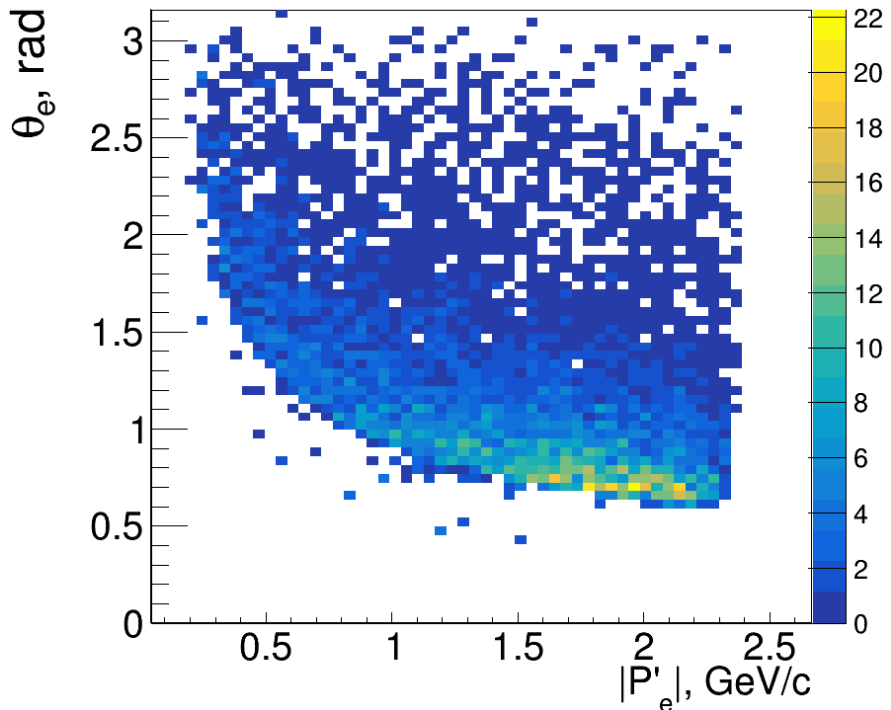
The estimation of  $e^+e^- \rightarrow \eta \gamma$  cross section based on the contribution of  $\rho$ ,  $\omega$ ,  $\phi$  mesons.



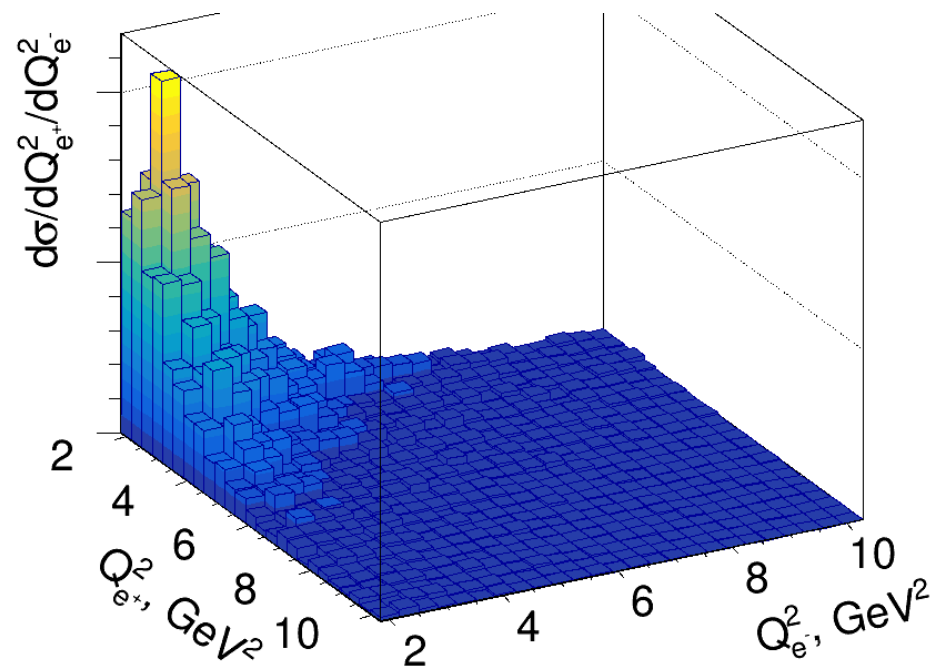
We need  $10 \text{ pb}^{-1}$ /point with VEPP-2000 at least for measurement of the cross section above  $\phi$  meson.

Let us consider the  $e^+e^-$  collisions at  $E_{\text{c.m.}} = 5 \text{ GeV}$ .

The obtained TFF allows us to predict  $\sigma_{e^+e^- \rightarrow e^+e^-\eta'}(Q_1^2, Q_2^2 > 2 \text{ GeV}^2) = 3.06 \pm 0.01 \text{ fb}$



*The angle vs momentum of scattered fermion*



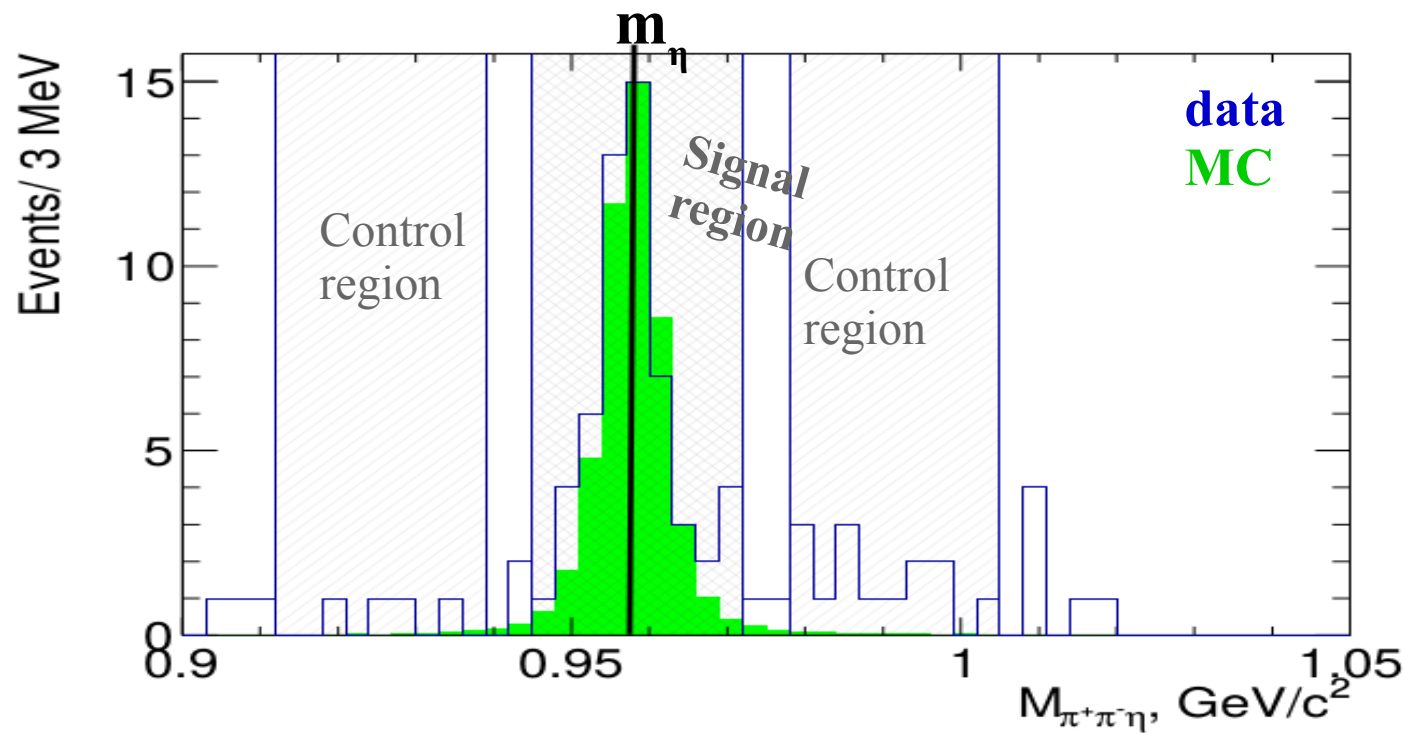
*The differential cross section*

The measurement of double off-shell TFF is a **challenge** and can be performed only at experiments with super high luminosity.



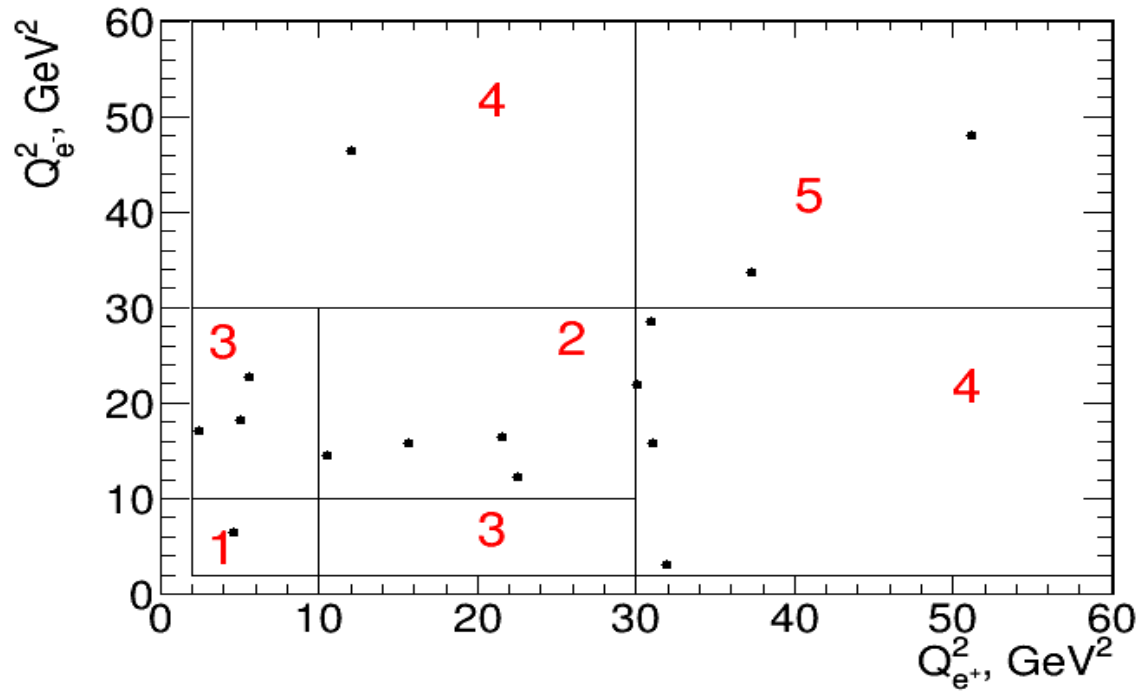
Thank you for your attention

Back up slides



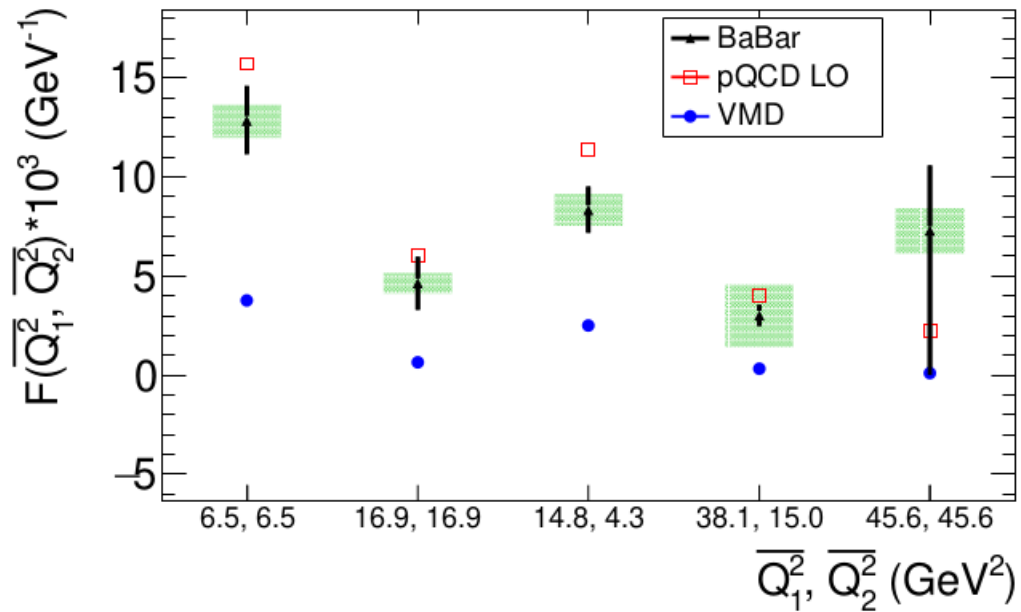
*The data-MC comparison of  $\pi\pi\eta$  invariant mass distribution. The MC histogram is normalized to central bin of data distribution.*

The expected number of signal  $N_{\text{signal}}^{\text{side}} = 55 - 18/2 = 46$



*The  $Q_{e-}^2$  vs.  $Q_{e+}^2$  for events from control side-band regions*

If  $(d^2\sigma/(dQ_1^2 dQ_2^2))_{MC}$  and  $\epsilon_{true}$  is made using VMD TFF:



*The comparison of obtained form-factor with theoretical predictions. The Error bars - statistical uncertainties. Shaded rectangles - quadratic sum of the systematic and model uncertainties.*

$$|\eta'\rangle = \sin\phi |n\rangle + \cos\phi |s\rangle$$

$$F_{\eta'} = \sin\phi F_n + \cos\phi F_s$$

$$\bullet \lim_{Q^2 \rightarrow \infty} F_n(Q^2) = \frac{5\sqrt{2}}{3Q^2} f_n; \lim_{Q^2 \rightarrow \infty} F_s(Q^2) = \frac{2}{3Q^2} f_s$$

$$|n\rangle = \frac{1}{\sqrt{2}}(|\bar{u}u\rangle + |\bar{d}d\rangle)$$

$$|s\rangle = |\bar{s}s\rangle$$

$$|\eta'\rangle = \sin\phi |n\rangle + \cos\phi |s\rangle$$

**Master formula**

$$\bullet F_{\eta'}(Q_1^2, Q_2^2) = \left( \frac{5\sqrt{2}}{9} \cdot f_n \cdot \sin\phi + \frac{2}{9} \cdot f_s \cdot \cos\phi \right) \cdot \int_0^1 dx \frac{3x(1-x)}{xQ_1^2 + (1-x)Q_2^2} \left( 1 + C_F \frac{Q^2}{2\pi} \cdot t(x, Q_1^2, Q_2^2) \right) + (x \rightarrow 1-x)$$

• at which scale of  $Q^2$  the asymptotic pQCD prediction starts to be valid?

• In the case of  $\gamma\gamma^* \rightarrow P$ :

$$F_{\eta'}(Q^2) = F_{\eta'}(Q^2, 0) = \frac{\frac{5\sqrt{2}}{9} \cdot f_n \cdot \sin\phi + \frac{2}{9} \cdot f_s \cdot \cos\phi}{Q^2} \cdot \left( 1 - \frac{5}{2} C_F \frac{\alpha_S(Q^2)}{2\pi} \right)$$